COMPOSITE PLATES WITH THROUGH-THICKNESS ALIGNED CARBON NANOTUBES

K. Dassios[1,2*], C. Galiotis[2,3]

[1] *Department of Materials Science and Engineering, University of Ioannina, Ioannina 45110, Greece*
[2]*Foundation for Research and Technology Hellas, Institute of Chemical Engineering Sciences, Stadiou Street, Platani, Patras GR-26504, Greece*
[3] *Department of Materials Science, University of Patras, Rio GR-26500, Greece*
**kdassios@cc.uoi.gr*

Keywords: carbon nanotubes, chemical vapor deposition, growth, nanocomposites

Abstract
Mats of uniformly-dispersed, vertically-aligned multiwall carbon nanotubes were grown in an environmentally-friendly thermal CVD reactor and soaked, without any prior chemical modification, into epoxy and PVA solutions to produce composite plates of z-axis nano-reinforcement. Direct observations of polymer-CNT interactions at the nanoscale revealed that both media interacted naturally with the CNTs without affecting their physical characteristics, vertical alignment, or the mat's morphology. The compressive behaviors of CNT/epoxy mats exhibited a triple regime behavior with the elastic regime being followed by elastic instability and compaction. Evidence of reinforcement was suggested by stiffness and toughness values significantly higher than the pure polymer. PVA-CNT interactions were strong with a 7 to 10-fold increase in the apparent nanotube diameter due to polymer sheathing. TGA measurement in the CNT/PVA showed a crystallinity increase of the polymer phase due to the presence of CNTs. Potential applications of the composites include filters, components for sandwich panels and sensors.

1 Introduction
Owing to their exceptional physical properties such as strength, toughness and high aspect ratios, carbon nanotubes (CNTs) [1], have emerged as the most promising 1D medium for modern composite systems. In the nanocomposite material family, the efficiency and homogeneity of CNT dispersion within the matrix material are of equally high importance as understanding and controlling the interfacial interactions occurring between the nano-reinforcement and the continuous phase. It is long now well established that CNTs have poor dispersibility in polymeric matrices unless their surface is previously chemically modified or elsewise functionalized [2]. Under this route, polymer matrix nanocomposites of -mainly- single CNT nanofibers have successively been manufactured [3-6] where the matrix material was mainly poly(vinyl alcohol) (PVA) [7-9] but also polypropylene and polyethylene [7, 10, 11]. Dalton *et al* reported the production of super tough PVA/SWCNT fibers of a 60 wt% SWCNT content, processed with the aid of a surfactant [9]. Indirect methods for homogeneously dispersing CNTs in polymeric media have also been reported [12-16] together with electric field [17], magnetic field [18],[19], electrospinning [20] and mechanical force [6],[14] methods of aligning nanotubes for the production of polymer nanocomposites

of custom isotropies. The majority of these studies employs the chemical oxidation/modification route to increase the affinity of the graphitic surface with the polymer; a route that may, under certain conditions, have negative side-effects on the tubes' physical, thermal and electrical properties [21-23]. Wardle *et al* have exploited the CNT-polymer capillary forces to successfully wet CNT forests by epoxy matrices via a submersion process without prior functionalization of the tubes [24, 25]. Very limited information is also available on the compressive properties of such vertically-aligned CNT nanocomposites [26-28]. Garcia *et al* reported a 220% increase in the modulus of a CNT/thermoset-epoxy matrix with respect to the dry product [28] while Ci *et al* claimed a corresponding 3300% increase in a polydimethylsiloxane-matrix nanocomposite [27]. A straightforward methodology for achieving custom nanoreinforcement morphology and orientation within the continuous polymer medium is still being sought, mainly due to the difficulty associated with handling nanotubes and nanofibres. On the other hand, a detailed investigation of the polymer sheathing phenomenon in polymer/CNT nanocomposites has yet to be undertaken. Understanding the interaction between the two phases and the impact of sheathing on the physical properties of the interphase region is key to characterizing the mechanical properties of nanocomposites [29].

We report here the manufacturing and main aspects of PVA- and epoxy- nanocomposites plates reinforced by vertically-aligned, millimeter-high CNTs. The composite were achieved by direct soaking, in the polymeric solutions, of millimetres-high, as-grown mats of vertically-aligned nanotubes, without having received any kind of chemical or physical modification. We found extensive polymer sheathing to have occurred throughout the product volume *without* alteration to the vertical alignment or morphology of the as-grown CNT mat. Moreover, the tubes' physical characteristics remain unaffected by the interaction with the polymer that fills the open porosity of the mat by coating annularly the tubes. The evidence presented herein includes (a) SEM and TEM imaging of the mats' volumes showing nanotubes coated annularly by PVA; (b) a 7 to 10-fold increase in the apparent nanotubes diameter due to sheathing measured at nanotube tips with protruding carbon cores and (c) TGA evidence supporting the argument that CNTs nucleate PVA crystallinity. The mechanical performance of epoxy-nanocomposite mats was studied in comparison to that of the as-grown CNT material. Possible applications of such nanocomposite mats include sandwich panel elements, electrochemical energy storage media, vibration absorbers, multifunctional and conductive composites applications.

2 Materials and testing methods

2.1 CVD growth of carbon nanotube mats

The CVD methodology employed in this study makes use of a simultaneous catalyst/carbon feed concept to overcome the limitations of catalyst saturation – hence also final product height – encountered in the conventional catalytic-CVD setups. Herein, the catalyst precursor, ferrocene and the carbon source, camphor, are introduced into the reactor in a common gas mixture so that, in the presence of fresh catalyst particles, carbon decomposition remains active for longer periods of time. The advantages of the simultaneous feed concept are manifold, as the technique allows for 1) synthesis of unconventionally high CNT mats, 2) use of bare substrates, as opposed to conventional catalyst-coated ones and 3) deposition on randomly-shaped substrates, as well as on non-silicon substrates. Another improvement to the conventional CVD setup is the burning of the gaseous product of the decomposition under open flame, before it is released to a HEPA-filter fume hood and then on to the environment. During this phase, the gas output is efficiently purged of phenanthrene, naphthalene and other polycyclic aromatic hydrocarbons (PAH). On the other hand, the CVD route employed for

synthesizing the CNT mats, based on commercial camphor, is economical, environmentally friendly and conforms with the 12 principles of green chemistry as issued by the United States Enviromental Protection Agency (US EPA) [30].

MWCNT mats were synthesized inside a 1.2m long quartz reactor, inner diameter 40mm, that was positioned horizontally in a three-zone split furnace (Fig. 1) operating with a nitrogen carrier gas flow. The catalyst and carbon sources, ferrocene and camphor respectively, were mixed in solid state (powder form) in a 1:20 ratio and transferred to a glass flask connected to the quartz reactor by means of a T-join. The reagents were evaporated with the help of a heater plate at 230^{o}C. Crystalline silicon plates of 1-0-0 crystal orientation, and dimensions of 150mm x 38mm x 0.725 mm (l x w x t), were inserted centrally along the reactor's length and serve as substrates for the deposition of CNTs. The surface of the substrates was initially cleaned with acetone. Introduction of precursors into the reactor was allowed once the reactor temperature was stabilized at 850^{o}C. Chemical vapour deposition of carbon nanotubes endured for ca. 60min and was terminated manually. Output gases were burnt under open flame before being released into a fume hood and then on to the environment. This step allowed removal of harmful polycyclic aromatic hydrocarbons (PAH), such as naphthalene and phenanthrene, produced during the deposition. To the authors' knowledge, this is the first CNT growth reactor to implement a purification of the output gases which is a step closer to a cleaner environment. Upon removal of the substrates, thick deposits (ca.2-2.5 mm in height for the stated experiment duration) of vertically-aligned MWCNTs were found on the Si wafers while the inner walls of the quartz reactor were also covered with thinner MWCNT layers. The MWCNT mats were separated from the Si wafers using a razor blade. The maximum growth rate for a 2.3mm-high final product was calculated at 0.7μm/sec.

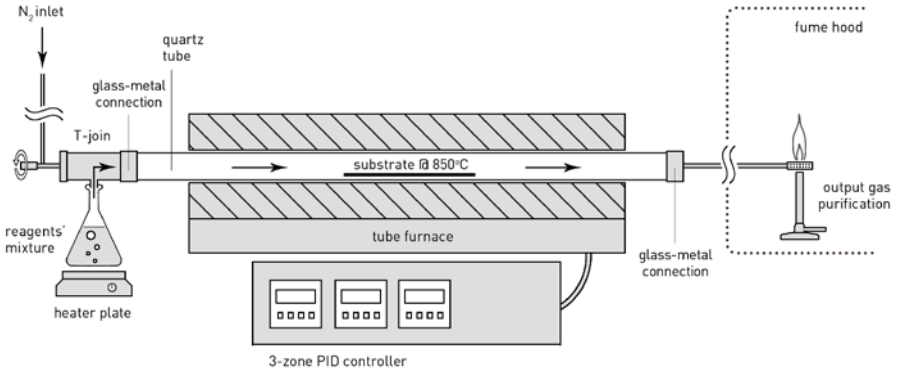

Figure 1. CVD setup for growth of vertically aligned MWCNTs

2.2 Manufacturing of nanocomposites

A plausible method to impregnate the as-deposited material with epoxy resin while avoiding the complexity and side effects of chemical functionalization of CNTs, was sought. Several unsuccessful attempts to impregnate the mats with the uncured matrix, including vacuum-assisted infusion under 10 bars of autoclave pressure, proved that the material was highly unfriendly to the polymer matrices, especially epoxy. An investigation of the wettability of the mats in different solvents, eventually proved that the highly hydrophobic as-grown material was particularly friendly to one specific solvent: acetone [31]. Mats floated on acetone would absorb the liquid and sink while releasing entrapped air in an effervescent manner. The established acetone-friendly characteristic was important because acetone is also a good solvent for the uncured epoxy resin. Thereafter, blocks of CNT mats were wet in acetone-thinned solutions of 10%, 30% and 50% b.w. of uncured epoxy that was prepared by mixing the curing agent and resin in a 58:100 weight ratio. Prior to soaking, the mats were

rinsed with an acetone flow to remove all excess carbon particles and surface debris. The mats were left to soak in the epoxy solutions for 1 hour; all effervescing activity appeared to cease already after 30 minutes into soaking. The mats were subsequently cured to the resin-specific cycle into a vacuum oven (Gallenkamp, Leicestershire UK); the cycle included a curing step at 80°C for 2 hours followed by post-curing at 130°C for 1 hour.Upon cooling to room temperature, the impregnated mats were stiff enough to be straightforwardly cut into any right shape with a sectioning saw.

Similarly, individual MWCNT mats of approximate dimensions 40mm x 35mm were soaked into pure acetone and then immersed into an aqueous 1%wt PVA solution for 1 hour. Acetone acts as an intermediate medium to render the material hydrophilic –hence friendly to the water-based PVA solution- while it removes excess air trapped within the pores of the MWCNT mat. The PVA-soaked samples were dried overnight in a vacuum oven.

2.3. Specimens and Testing

Compression specimens were prepared by cutting epoxy-impregnated mats into rectangular parallelepipeds of cross sectional areas of 15-20mm^2 using a diamond wafering blade (Diamond Blade, Medium Grit, Medium Concentration, Ted Pella Inc., California, USA) on a low-speed precision sectioning saw (Buehler Isomet Low Speed Saw, Buehler Ltd, Illinois, USA). The height of the resulting composite plates remained equal to the as-grown value, 1.5-2.5 mm. Similar specimens were also prepared for the pristine material by sectioning the pure CNT mats with a razor blade. The cross sectional area of the latter specimens was approximately 25mm^2. To establish the compressive behavior of the matrix material independently, samples of pure epoxy were prepared by casting a 58:100 weight mixture of Epikure agent and Epikote resin in a Teflon assemblage providing an internal block volume of 20x20x30 mm^3. Vacuum was used to compact the mixture for a period of 15min. The system was then cured to the resin-specific cycle, following a procedure identical to the impregnated mats. Pure resin slices of cross sectional areas of 75-85mm^2 and heights of 2.3-2.4 mm (comparable to the composite mats) were cut from the block using the aforementioned sectioning equipment.

Specimens of pure resin, as-grown MWCNT mats and epoxy-impregnated nanocomposite mats were tested in compression in an Instron® 5900 Electromechanical testing frame(Instron Industrial Products, Pennsylvania, USA) equipped with a 100kN load cell. Testing was performed in cross-head displacement control with a strain rate of0.1min^{-1}.

PVA/MWCNT nanocomposite plates were cut into *ca.* 10mmx10mm pieces to be examined by Scanning Electron Microscopy, Transmission Electron Microscope and Thermo-Gravimetric Analysis. For TEM analysis, the PVA/MWCNT fibers were dispersed in DMF and sonicated for 5 minutes. Then a droplet of the solution was applied on a TEM copper/carbon grid. The grid was left to dry overnight at room temperature.

3 Results and Discussion

After separation from the silicon substrate, the as-grown MWCNT mats were self-standing and of macroscopic dimensions. Mat microstructure was investigated by SEM. As seen in Fig.2, tube growth was predominantly vertically-oriented (Fig.2a) while a certain degree of inter-CNT entanglement became prominent in higher magnifications (Fig. 2b). This branching is responsible not only for the free-standing integrity of the mat, but also for its potential, under certain conditions, to be drawn and twist-spun into CNT yarns.

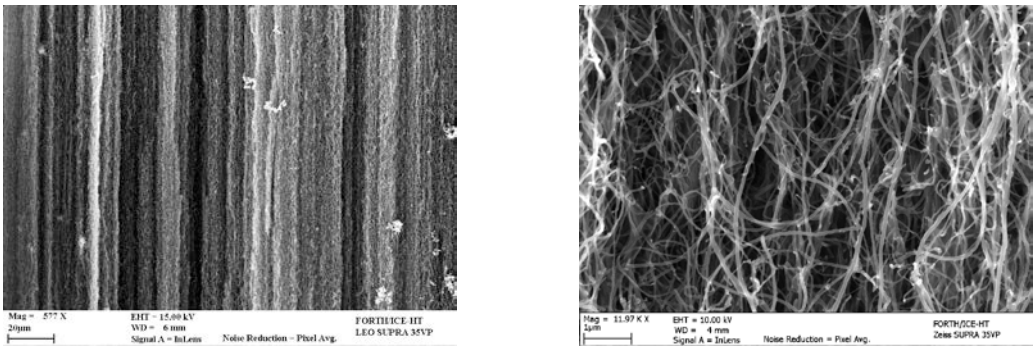

a. **b.**

Figure 2: SEM micrographs of the as-grown MWCNT mats a) Low magnification image demonstrating the dominant vertical arrangement of the tubes, b) Higher magnifications reveal branching between MWCNTs

CNT diameter in the as-grown material ranged from 30 to 70 nm whereas the density of the mats was calculated at 0.35 g·cm^{-3}. The pore structure of the as-deposited mats was analyzed in a PoreMaster® 60 mercury porosimeter (Quantachrome Instruments, Florida, USA). A highly uniform pore distribution was observed with 88% of the pores ranging around a mean diameter of 0.4μm with a standard deviation of 0.34μm while 9% and 3% of the pores were found at 17μm and 170μm respectively. These findings indicate that MWCNTs were homogeneously dispersed throughout the volume of the mat which we believe is important in view of a) the well-documented difficulty of other methods to achieve similar CNT homogeneity and b) of the uniformity required in the target composite system. The void fraction of the material was also established by porosimetry to be 0.73.

The void space coverage efficiency of the epoxy was examined under SEM by observation of cross-sections of composite mats soaked into solutions of varying resin concentration. Fig. 3a, b and c, demonstrate the typical topology of mats soaked in 10%, 30% and 50% b.w. solutions, respectively. In the thinner 10% and 30% solutions epoxy was uniformly dispersed throughout the volume of the material and mixed well with the CNTs, forming, where available, well-defined menisci between CNTs(Fig. 3a and b). However, it only provided partial coverage of the void space. Complete void coverage was achieved with the 50% by weight epoxy solution (Fig. 3c) as established by porosimetry. Fig. 3 also demonstrates that the homogeneity and vertical orientation of CNTs in the mat remained unaffected by the interaction with the polymer or by the thermal curing procedure.

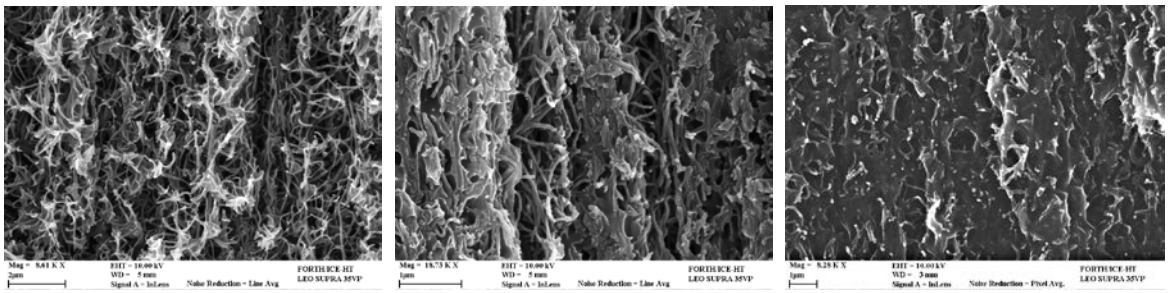

a. **b.** **c.**

Figure 3: Degree of void space coverage offered by various concentrations of epoxy: a)10, b)30 and c)50%wt

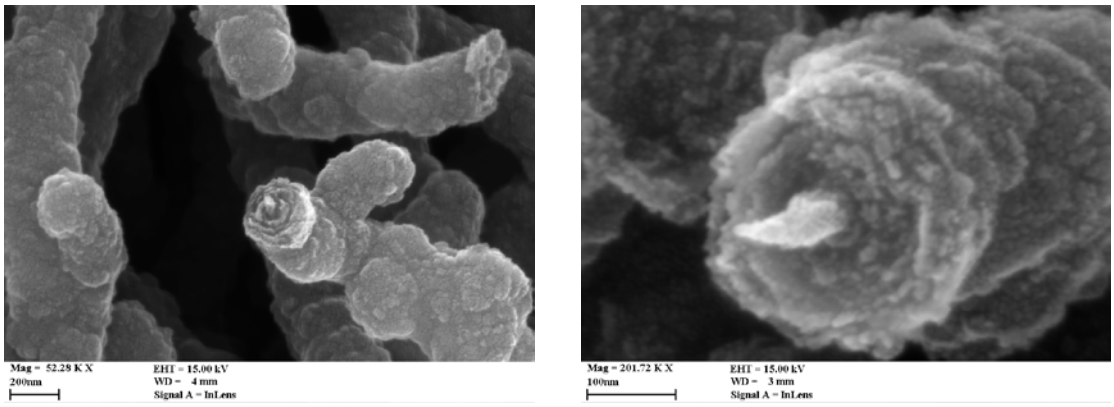

a. b.

Figure 4: PVA-coated CNTs in the nanocomposite with close-up of tips showing layers of PVA absorbed around the tube core.

The typical morphology of the PVA nanocomposite, as captured by SEM, is presented in Fig. 4. The first observation that emerged from the morphological examination of the composite mats was that the surface of CNTs was the preferable location for absorption of PVA; polymer coagulates were not found in other locations. This means that the presence of the tubes did not allow the polymer to self-coagulate independently, as in the case of epoxy. Secondly, PVA appeared to have deposited at annular layers around the tubes' surface, starting from the CNT surface; this observation was made possible at the free tips of PVA-coated tubes where concentric layers of polymer sheaths were visible around protruding cores of carbon nanotubes (Fig. 4b). CNT diameter in the PVA-nanocomposite mat was measured at approximately 300nm, which is seven to ten timed greater than the as-grown tubes diameter. This "magnification" factor range has a significant engineering interest as it essentially controls the open porosity of the composite/hybrid material. This factor is controlled by the PVA concentration in the aqueous solution, which also controls the thickness of the polymer sheathe around the tubes A third observation was that the presence of PVA did not promote coalescence of the nanotubes themselves nor changed the vertical alignment and morphology of the as-grown mat. A similar behaviour has also been reported by Zhang et al [4].

Thermogravimetric analysis (TGA) was employed to investigate the crystallinity and thermal response of the PVA/CNT nanocomposite as well as its constituents: i) as-grown CNT carpet and ii) PVA in granule form (as received). As seen in Fig. 5, owing to its fine structure, the as-grown carpet has the greatest thermal stability among the three materials. On the other hand, the PVA mass loss curve shows that the polymer has the lowest thermal stability, a property common to linear polymers of low molecular weight. The PVA curve exhibits two degradation stages: The first one at 300 °C is related to the elimination of the amorphous parts of the polymer while the second one, at 400 °C, corresponds to the degradation of the higher thermal stability crystalline parts.

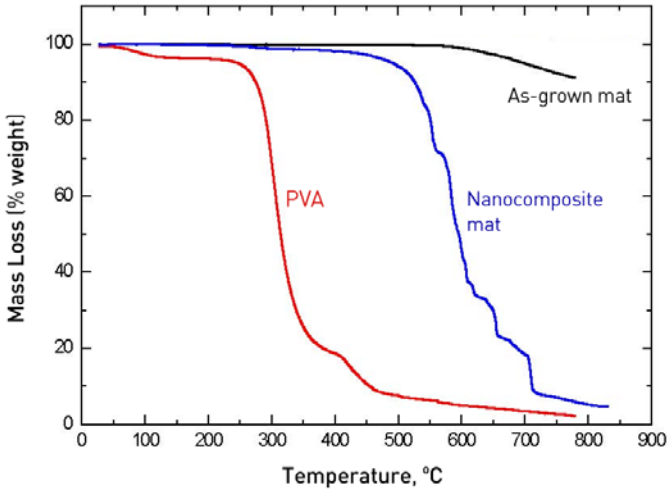

Figure 5. Mass change curves for the polymer, pristine CNT mat and nanocomposite mat.

The nanocomposite's mass loss curve exhibited 5 steps of degradation: two significant drops at 520°C and 710°C and 3 intermediate steps at 580 °C, 620 °C and 650°C of less intensity. The first step, at 520°C is related to the decomposition of amorphous PVA parts, while the remaining multi-step behaviour can be attributed to the nucleated PVA crystallinity due to the presence of CNTs. Similar findings have been offered in the past for PVA/CNT mixtures of weight fractions as low as 0.1% [9] as well as for other polymers [32-34]. If crystallinity increases with decreasing nanotube diameter [4], the observed multi-step behaviour can be associated with crystallinity ranging from its highest value on small-diameter CNTs, to its lowest value at the outer layers of thicker tubes. Of course the diameter and crystallinity distributions are not discrete but continuous and therefore a one-to-one relation between mass drops in the TGA curve and the two affecting parameters should not be expected. This may explain the generally uneven form of the composite's TGA curve in (Fig. 5). Nonetheless, it should be reminded that the PVA coating procedure did not involve thermal annealing, a procedure that could independently increase the degree of crystallinity of the polymer. Hence the observed crystallinity nucleation is the sole result of the presence of CNTs.

The compressive behavior of the vertically-aligned-MWCNT/epoxy composites was compared to their as-grown counterparts. The calculation of stress for the pristine material took into account the 0.27 CNT volume fraction that was calculated by porosimetry, whereas composite stress was calculated based on the total specimen cross section. The typical stress-strain behavior of pristine and composite mats is presented in Fig. 6 by the dashed and straight lines respectively, while the response of pure epoxy specimens is represented by a dotted line. The mechanical response of all three materials was consistent with the triple regime behavior (elastic/instable/plastic) expected by conventional mechanics for compression of identical beams entrapped between two parallel horizontal plates. Therein, the elastic regime endures for axial loads up to the critical Eulerian buckling load for the beams, at which point elastic instability occurs, giving rise to a plastic contribution. The Euler load - hence also the stress of the beams- remains practically constant throughout the instability regime, which endures up to the compaction mechanism that starts with the first nanotube fracture. This final regime is related with very steep stress-strain behavior, comparable to the single-tube value.

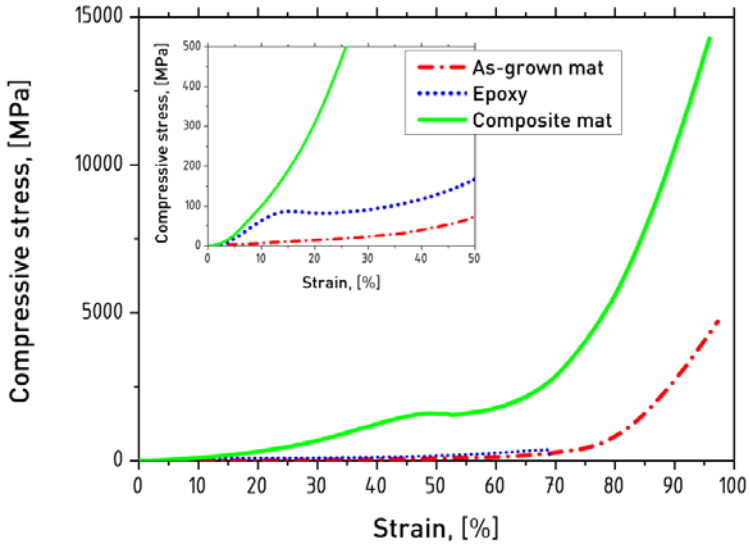

Figure 6: Compressive behavior of epoxy and the as-grown and nanocomposite mats

The pure polymer showed a typical linear behavior up to 12% strain,consistent with a modulus of 1.2 GPa and a failure strength of 90 MPa. The as-grown CNT mats exhibitedquite low Young's moduli of ca. 80MPa, which are considerably higher than previously quoted values of 0.25MPa [35] and 4.5MPa [36] for similar materials under compression. The corresponding modulus for the composite mat was 1.5 GPa, approximately 25% higher than the pure polymer modulus and 1800% higher than the as-grown mats' modulus. Instability in the epoxy resin occurred at ca.12% strain -at which point the material had evidently failed- while compaction at ca. 50% strain. Both pristine and composite mats did not exhibit elastic instability up to 35% strain while nanotube fracture became significant at 75% and 60% strain for the pristine and composite materials respectively. By comparison it was noted that plasticity appears in the epoxy composite at three times higher strain than in the pure resin itself. Identifying the value of stress on the onset of compaction as the materials' strength for the given test configuration, we obtain values of 425 MPa and 1600 MPa for the as-grown and composite mats respectively. This 4-fold increase in strength is compatible with the existence of reinforcement.

5. Conclusions

PVA- and Epoxy- nanocomposite plates were produced by soaking millimetres-high CVD-grown carpets of vertically-aligned nanotubes into aqueous and acetonic solutions of the two polymeric matrices, respectively. The carpets were initially rendered hydrophilic by a simple process that involved wetting with acetone alone. Extensive polymer-CNT interaction in the form of polymer sheathing was directly observed in the nanoscale under SEM. The polymers did not interfere with the internal structure of the grown carpets and the tubes' physical characteristics remained unaltered by the sheathing mechanism. CNT were coated annularly by PVA while epoxy appeared to coalesce independently of filler topology. TGA analysis of the PVA-nanocomposites was compatible with crystallinity increase as a sheer result of the presence of the tubes. The compressive behavior of the as-growth mats as well as the epoxy-nanocomposites was, in accordance with theoretical predictions, compatible with the classic triple-regime response that includes elastic behavior, instability and compaction. The findings of a 20-fold increase in Young's modulus and 4-fold increase in the strength of the composite with respect to the as-grown case, clearly indicated the effect of reinforcement in compression for the MWCNT/epoxy mats studied here.

References

[1] Iijima, S., et al., *Structural flexibility of carbon nanotubes.* Journal of Chemical Physics, 1996. **104**(5): p. 2089-2092.
[2] Datsyuk, V., et al., *Chemical oxidation of multiwalled carbon nanotubes.* Carbon, 2008. **46**(6): p. 833-840.
[3] Ryan, K.P., et al., *Carbon nanotubes for reinforcement of plastics? A case study with poly(vinyl alcohol).* Composites Science and Technology, 2007. **67**(7-8): p. 1640-1649.
[4] Zhang, X.F., et al., *Poly(vinyl alcohol)/SWNT composite film.* Nano Letters, 2003. **3**(9): p. 1285-1288.
[5] Zhang, X.F., et al., *Gel spinning of PVA/SWNT composite fiber.* Polymer, 2004. **45**(26): p. 8801-8807.
[6] Vigolo, B., et al., *Macroscopic fibers and ribbons of oriented carbon nanotubes.* Science, 2000. **290**(5495): p. 1331-1334.
[7] Ryan, K.P., et al., *Multiwalled carbon nanotube nucleated crystallization and reinforcement in poly (vinyl alcohol) composites.* Synthetic Metals, 2006. **156**(2-4): p. 332-335.
[8] Xue, P., et al., *Electrically conductive yarns based on PVA/carbon nanotubes.* Composite Structures, 2007. **78**(2): p. 271-277.
[9] Dalton, A.B., et al., *Super-tough carbon-nanotube fibres - These extraordinary composite fibres can be woven into electronic textiles.* Nature, 2003. **423**(6941): p. 703-703.
[10] Probst, O., et al., *Nucleation of polyvinyl alcohol crystallization by single-walled carbon nanotubes.* Polymer, 2004. **45**(13): p. 4437-4443.
[11] Bhattacharyya, A.R., et al., *Crystallization and orientation studies in polypropylene/single wall carbon nanotube composite.* Polymer, 2003. **44**(8): p. 2373-2377.
[12] Barrera, E.V., *Key methods for developing single-wall nanotube composites.* Jom-Journal of the Minerals Metals & Materials Society, 2000. **52**(11): p. A38-A42.
[13] Schadler, L.S., S.C. Giannaris, and P.M. Ajayan, *Load transfer in carbon nanotube epoxy composites.* Applied Physics Letters, 1998. **73**(26): p. 3842-3844.
[14] Jin, L., C. Bower, and O. Zhou, *Alignment of carbon nanotubes in a polymer matrix by mechanical stretching.* Applied Physics Letters, 1998. **73**(9): p. 1197-1199.
[15] Yang, K., et al., *Effects of carbon nanotube functionalization on the mechanical and thermal properties of epoxy composites.* Carbon, 2009. **47**(7): p. 1723-1737.
[16] Liu, W., et al., *Producing superior composites by winding carbon nanotubes onto a mandrel under a poly(vinyl alcohol) spray.* Carbon, 2011. **49**(14): p. 4786-4791.
[17] Zhu, Y.F., et al., *Alignment of multiwalled carbon nanotubes in bulk epoxy composites via electric field.* Journal of Applied Physics, 2009. **105**(5).
[18] Kimura, T., et al., *Polymer composites of carbon nanotubes aligned by a magnetic field.* Advanced Materials, 2002. **14**(19): p. 1380-1383.
[19] Chiolerio, A., et al., *Preparation of polymer-based composite with magnetic anisotropy by oriented carbon nanotube dispersion.* Diamond and Related Materials, 2008. **17**(7-10): p. 1590-1595.
[20] Sen, R., et al., *Preparation of single-walled carbon nanotube reinforced polystyrene and polyurethane nanofibers and membranes by electrospinning.* Nano Letters, 2004. **4**(3): p. 459-464.
[21] Zhang, J., et al., *Effect of chemical oxidation on the structure of single-walled carbon nanotubes.* Journal of Physical Chemistry B, 2003. **107**(16): p. 3712-3718.
[22] Liu, C.H. and S.S. Fan, *Effects of chemical modifications on the thermal conductivity of carbon nanotube composites.* Applied Physics Letters, 2005. **86**(12).
[23] Garg, A. and S.B. Sinnott, *Effect of chemical functionalization on the mechanical properties of carbon nanotubes.* Chemical Physics Letters, 1998. **295**(4): p. 273-278.
[24] Wardle, B.L., et al., *Fabrication and characterization of ultrahigh-volume-fraction aligned carbon nanotube-polymer composites.* Advanced Materials, 2008. **20**(14): p. 2707-+.
[25] Garcia, E.J., et al., *Fabrication of composite microstructures by capillarity-driven wetting of aligned carbon nanotubes with polymers.* Nanotechnology, 2007. **18**(16).

[26] Thostenson, E.T. and T.W. Chou, *On the elastic properties of carbon nanotube-based composites: modelling and characterization.* Journal of Physics D-Applied Physics, 2003. **36**(5): p. 573-582.
[27] Ci, L., et al., *Continuous carbon nanotube reinforced composites.* Nano Letters, 2008. **8**(9): p. 2762-2766.
[28] Garcia, E.J., et al., *Fabrication and nanocompression testing of aligned carbon-nanotube-polymer nanocomposites.* Advanced Materials, 2007. **19**(16): p. 2151-+.
[29] Spitalsky, Z., et al., *Carbon nanotube-polymer composites: Chemistry, processing, mechanical and electrical properties.* Progress in Polymer Science, 2010. **35**(3): p. 357-401.
[30] Anastas, P.T. and J.C. Warner, *Green chemistry : theory and practice*. 1998, Oxford England ; New York: Oxford University Press. xi, 135 p.
[31] Dassios, K. and C. Galiotis, *Polymer-nanotube interaction in MWCNT/poly(vinyl alcohol) composite mats.* Carbon, 2012.
[32] Xie, X.L., et al., *Ultrahigh molecular mass polyethylene/carbon nanotube composites - Crystallization and melting properties.* Journal of Thermal Analysis and Calorimetry, 2003. **74**(1): p. 317-323.
[33] Sandler, J., et al., *Crystallization of carbon nanotube and nanofiber polypropylene composites.* Journal of Macromolecular Science-Physics, 2003. **B42**(3-4): p. 479-488.
[34] Grady, B.P., et al., *Nucleation of polypropylene crystallization by single-walled carbon nanotubes.* Journal of Physical Chemistry B, 2002. **106**(23): p. 5852-5858.
[35] Tong, T., et al., *Height independent compressive modulus of vertically aligned carbon nanotube arrays.* Nano Letters, 2008. **8**(2): p. 511-515.
[36] Musso, S., et al., *Improving macroscopic physical and mechanical properties of thick layers of aligned multiwall carbon nanotubes by annealing treatment.* Diamond and Related Materials, 2008. **17**(4-5): p. 542-547.